

# ATOM: Efficient On-Device Video-Language Pipelines Through Modular Reuse

Kunjal Panchal<sup>1</sup>, Saayan Mitra<sup>2</sup>, Somdeb Sarkhel<sup>2</sup>, Haoliang Wang<sup>2</sup>, Ishita Dasgupta<sup>2</sup>, Gang Wu<sup>2</sup>, Hui Guan<sup>1</sup>

<sup>1</sup>University of Massachusetts, Amherst <sup>2</sup>Adobe Research

## Abstract

Recent advances in video-language models have enabled powerful applications like video retrieval, captioning, and assembly. However, executing such multi-stage pipelines efficiently on mobile devices remains challenging due to redundant model loads and fragmented execution. We introduce ATOM, an on-device system that restructures video-language pipelines for fast and efficient execution. ATOM decomposes a billion-parameter model into reusable modules, such as the visual encoder and language decoder, and reuses them across subtasks like captioning, reasoning, and indexing. This reuse-centric design eliminates repeated model loading and enables parallel execution, reducing end-to-end latency without sacrificing performance. On commodity smartphones, ATOM achieves 27–33% faster execution compared to non-reuse baselines, with only marginal performance drop ( $\leq 2.3$  Recall@1 in retrieval,  $\leq 1.5$  CIDEr in captioning). These results position ATOM as a practical, scalable approach for efficient video-language understanding on edge devices.

## 1 Introduction

Video-language model (VLM) pipelines (Jo et al. 2024; Yan et al. 2025; Long et al. 2025) are rapidly becoming the engine behind emerging mobile applications such as on-device video retrieval (Tahboub, Gadgil, and Delp 2015; Zhang et al. 2021) and video assembly (Yang et al. 2023), where users locate or stitch together video clips through natural-language prompts. Such applications rely on multi-stage pipelines that typically involve three core subtasks: video encoding, caption generation, and downstream reasoning or indexing. Running these pipelines locally is highly desirable because it preserves privacy and does not require a cloud server infrastructure.

However, deploying VLM pipelines on mobile devices presents fundamental challenges due to both memory and latency constraints. In standard pipelines, subtasks such as video encoding, caption generation, and script generation are handled by separate models (Yang et al. 2023; Xu et al. 2023c), each requiring its own memory footprint and processing time. For instance, even after applying 8-bit quantization, mPLUG2 (Xu et al. 2023b), a model commonly used for video-to-caption generation, requires approximately 5.6GB of RAM. Adding a script-generation model such as Llama 3.2 can consume an additional 1.4GB.

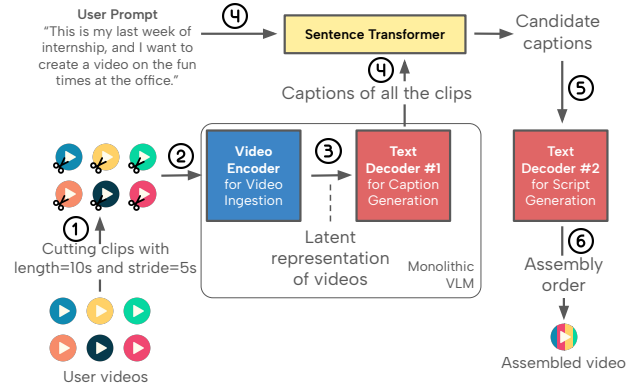
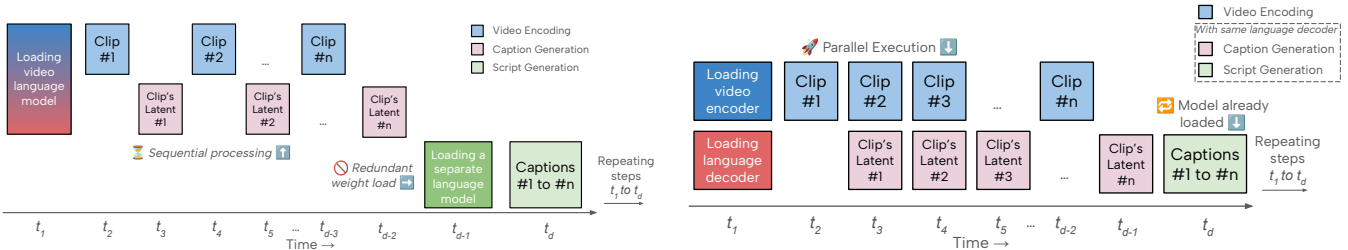


Figure 1: An end-to-end on-device sequential pipeline for video assembly. Given (i) user videos and (ii) a user prompt, the pipeline converts all the video clips into their text representations, generates a script and assembles selected video clips accordingly.

Running the full pipeline would therefore require around 7GB of memory, which can strain mobile devices that typically have only 6 to 8GB of RAM. As a result, models used in the pipeline are loaded sequentially at each stage, as shown in Figure 1. This back-to-back loading prohibits pipelined execution across tasks and inflates end-to-end latency. Empirically, we observe up to a 17% increase in latency when reloading quantized versions of these models between subtasks. This inefficiency not only prolongs wait time but also limits scalability across multiple user prompts, where each prompt restarts the model-loading cycle.

Prior works have predominantly optimized individual model performance: accelerating token generation or reducing memory consumption per model (Chu et al. 2023; Li and Li 2023; Xu et al. 2025). While effective in improving pipeline performance, such efforts overlook *pipeline-level inefficiencies* inherent to chaining multiple subtasks. In a conventional video assembly pipeline (Figure 2a), all video clips are first passed through the video encoder and caption generator before a separate script generator is invoked. This serialized execution means (1) the shared VLM cannot process the next batch of video clips while script generation is still running, and (2) the use of a standalone script-generation model imposes a memory tradeoff: either keep



(a) Sequential execution in de facto pipelines. Subtasks are executed one after another, with separate models loaded at each stage (e.g., at  $t_1$  and  $t_{d-1}$ ), resulting in higher latency and memory overhead.

(b) Modular, reuse-centric, and parallel execution in ATOM. It reduces pipeline latency by modularizing the video encoder and language decoder; and parallelizing their execution across different inputs (e.g., starting at  $t_3$ ).

Figure 2: Sequential (left) vs. ATOM’s modular-parallel (right) pipeline execution.

both models in memory (which may exceed device limits) or pay the overhead of loading them sequentially. These limitations amplify latency and hinder responsiveness on edge devices. Overcoming them requires a modular, reuse-centric execution model that enables parallelism across inputs and subtasks.

**Our Approach.** We propose ATOM, a reuse-centric inference system that accelerates video-language pipelines by addressing the pipeline-level inefficiencies. Unlike the sequential baseline, which uses separate models for each subtask in the pipeline, our approach leverages a single modularized model architecture that supports all subtasks, enabling end-to-end reuse without compromising model quality. Specifically, ATOM decomposes the VLM into persistent and reusable modules: a video encoder and a generalizable language decoder, both of which remain resident in memory throughout the application’s lifetime. By reusing these modules across subtasks and avoiding repeated model loading, ATOM eliminates data movement overhead and enables parallel execution without increasing memory usage. This reuse-centric design is compatible with existing model compression techniques, offering additional opportunities to reduce memory consumption.

Figure 2 contrasts this reuse-centric design with the de facto multi-model baseline. In the status quo (Figure 2a), each video clip triggers a strictly serial workflow: the device first loads a monolithic encoder-decoder pair to generate captions sequentially for each video clip and then bring in a separate language model for script generation. Our approach (Figure 2b) decomposes a VLM into separately callable encoder and decoder modules that operate concurrently: while the decoder produces captions for clip #1, the encoder can already process clip #2. Then the same decoder is used for processing all the captions for generating a script for video assembly. This modular parallelism reduces cumulative model-loading time and boosts hardware utilization without increasing the memory footprint, delivering substantial end-to-end speed-ups on mobile devices.

**Empirical Results.** We evaluate ATOM on two representative video-language tasks (video retrieval and video assembly) on commercial mobile devices including the Google Pixel 5a, Pixel 8a, and Samsung Galaxy S23. Compared to conventional multi-model pipelines, ATOM (a) re-

duces model loading latency by up to 50%; (b) achieves up to 33% lower end-to-end latency through reuse and parallelism; (c) maintains competitive output quality with only marginal differences in performance metrics (e.g., 1.3–2.3 drop in Recall@ $k$  for retrieval, 0.6–1.5 drop in CIDEr for captioning); and (d) keeps peak memory virtually unchanged (only 0.76%  $\approx$  40MB higher than the baseline) while using a stronger, reusable text decoder that still fits within a 6GB smartphone RAM budget. While our evaluation focuses on video retrieval and video assembly, the reuse-centric pipeline design introduced by ATOM is broadly applicable to a wide range of video-language applications, including summarization, question answering, and temporal event localization.

This work makes the following contributions:

- We propose a reuse-centric pipeline design that highlights a new system-level direction for efficient video-language inference. The design accelerates video-language inference by sharing a single model’s internal modules across subtasks. This eliminates the overhead of managing multiple models during execution.
- We develop ATOM, a mobile inference system that enables the execution of full video-language pipelines on-device without relying on server infrastructure.
- We evaluate ATOM on real-world smartphones and demonstrate significant latency reductions and system-level efficiency improvements while preserving high output quality across tasks.

## 2 Related Works

We organize related work into two categories: (1) on-device inference for vision-language models (VLMs) and their deployment strategies, and (2) pipelines for video-centric tasks such as assembly and retrieval. ATOM bridges these areas through a reuse-centric design that improves end-to-end latency for video-language pipelines on mobile devices.

**On-device Vision-Language Models.** Recent work has explored adapting VLMs for mobile hardware. MOBILEVLM (Chu et al. 2023) and SPOTLIGHT (Li and Li 2023) demonstrate that billion-parameter VLMs can run efficiently on smartphones by pairing lightweight visual encoders with language decoders. However, these efforts primarily target image-based tasks and assume single-stage in-

ference. They do not address the challenge of executing multi-stage pipelines, where repeated model loading and lack of reuse can introduce substantial latency overhead. ATOM complements these efforts by focusing on architectural reuse within the pipeline to accelerate full-stack video-language inference on-device, rather than optimizing individual models in isolation.

**Video-Centric Pipelines.** Video-language tasks such as assembly and retrieval typically rely on modular pipelines composed of separate models for video encoding, captioning, and reasoning (Yang et al. 2023; Xu et al. 2023c). While effective, this approach incurs high runtime overhead, particularly on mobile devices, due to the need to repeatedly load and execute distinct models for each subtask into limited memory. For video assembly, methods like RATV (Yang et al. 2023) and TV-MGI (Yin et al. 2024) align video segments to human-written scripts using powerful server-hosted models. These approaches assume expert-written inputs and high-resource environments. ATOM, by contrast, automates both script generation and clip selection directly on-device using a unified model, making the process more accessible to end users. In video retrieval, prior work such as CLIP4CLIP (Luo et al. 2021) and FROZEN (Bain et al. 2021) relies on embedding-based alignment between video and text. More recent methods (Xu et al. 2023c; Jeong et al. 2025) integrate LLM-based reasoning to enhance retrieval quality, but depend on large proprietary models and cloud infrastructure. These methods are not deployable in resource-constrained or privacy-sensitive settings. ATOM shows that retrieval, assembly, and captioning can all be supported within a single reusable model on mobile devices, eliminating the need for cloud-based processing or manual supervision.

### 3 Design of ATOM

ATOM accelerates video-language pipeline inferences by eliminating pipeline-level redundancies through three key design principles:

- *Modularization*: A VLM is split into a video encoder and a stronger, reusable language decoder, each independently callable for reuse and concurrent execution.
- *Reuse*: Modules are persistently kept in memory and shared across subtasks, avoiding repeated loading.
- *Parallelism*: Decoupled modules enable thread-safe parallel execution, improving throughput and device utilization.

#### 3.1 Modular Execution of VLM Pipelines

In traditional monolithic VLM pipelines (Yang et al. 2023), tasks such as video captioning and script generation (shown in Figure 1) are implemented using separate models or tightly coupled end-to-end models. This results in high latency due to serialized execution and repeated model reloading. Moreover, monolithic VLMs prevent concurrent execution of different subtasks.

ATOM addresses these inefficiencies through modular decomposition. The video encoder and text decoder components of the VLM are exposed as independently callable

modules. This allows concurrent execution, for example, encoding a new video clip while simultaneously decoding captions from prior clips. A further benefit of modularization is that the *same* high-capacity language decoder can be reused across all text-centric stages. Replacing multiple specialized, lighter decoders with a single shared decoder (i) eliminates repeated model loading, (ii) promotes generalization by applying a stronger linguistic prior across all text-centric subtasks (e.g., captioning, retrieval indexing, script generation), and (iii) crucially, enables the entire pipeline to run within tight mobile memory budgets. In contrast, pipelines that tries to load together separate models for captioning and script generation often exceed the 6GB RAM limit on common smartphones. Our reuse of a single high-capacity decoder avoids this constraint while still improving quality. Empirical comparisons are reported in Section 5.2.

#### 3.2 Persistent Module Reuse

Even with modularization, sequential implementations that rely on task-specific models may reload different modules at each stage of a multi-stage pipeline, wasting compute and memory bandwidth. ATOM avoids this overhead through a *persistent reuse strategy*, keeping key modules; such as the video encoder and a stronger, unified language decoder, loaded in memory across tasks. For example, the same decoder used for caption generation is also reused for script composition, eliminating the need to load a separate language model for the latter stage.

This reuse strategy reduces latency and avoids memory thrashing under constrained resources. As shown in Figure 2a, non-reuse pipelines incur significant delays from repeated model loading and unloading, especially when using large language decoders. In contrast, ATOM (Figure 2b) retains modules in memory throughout execution, streamlining transitions across subtasks and ensuring smoother operation on mobile hardware.

Although the memory footprint of model weights and activations is comparable between implementations, reuse-centric design lowers auxiliary memory usage (e.g., temporary allocations during weight loading). The detailed memory breakdown is provided in Appendices F.4 and F.5.

#### 3.3 Parallelism through Modular Design

A key advantage of modularizing the VLM is enabling *parallel execution* of subtasks, something infeasible with monolithic or tightly coupled models. Traditional video-language pipelines enforce serialized execution due to thread-unsafe or memory-intensive models: caption generation must wait for video encoding to finish, and script generation must wait for captioning to complete. This leads to under-utilization of compute resources and increased end-to-end latency.

In contrast, ATOM’s decoupled encoder and decoder are exposed as independently callable, thread-safe modules that persist in memory throughout execution. This persistent modular design allows pipeline stages to overlap: for example, while the decoder generates captions for clip #1, the encoder can begin processing clip #2. Figure 2b illustrates how overlapping compute windows boosts throughput and improves hardware utilization on edge devices.

While this parallel execution increases peak activation memory, we show in Appendix F.4 that ATOM offsets this by eliminating temporary memory overhead from repeated model loading, resulting in only 40MB higher overall usage.

**Applicability to Other Tasks.** While our analysis focuses on video retrieval and assembly for concreteness, the modular and reuse-centric design in ATOM generalizes to other video-language tasks, including summarization, and question answering. We demonstrate this with additional task implementation outlines described in Appendix B.

## 4 Implementation of ATOM

We implement ATOM on top of the vision-language foundation model mPLUG2 (Xu et al. 2023b). We modularize its components to support persistent module reuse and parallel execution, enabling efficient on-device inference.

We choose mPLUG2 for three reasons: (a) it has demonstrated strong performance in video-language tasks like captioning and retrieval (Wu et al. 2024; Chen et al. 2024; Wang et al. 2024), (b) it is open-source and modular, allowing targeted architectural changes, and (c) it is compatible with quantization and serialization frameworks such as TorchAO (torchao 2024) for mobile deployment. The original mPLUG2 consists of a BERT-based text encoder and decoder (0.3B parameters each), a CLIP-ViT/L-14 visual encoder (0.4B), and a fusion module (0.5B), totaling 1.5B parameters. However, it is not optimized for task-level reuse: the decoder requires separate fine-tuning for different language tasks (e.g., captioning vs. script generation), increasing training and runtime overhead.

To enable reuse across subtasks, we make two key modifications. First, we discard the text encoder and fusion module, which are not required for our tasks. Second, we replace the BERT-based decoder with a 1B parameter Llama 3.2-based autoregressive decoder (Grattafiori et al. 2024). This decoder generalizes across captioning and reasoning tasks, allowing the same module to serve both roles without re-training.

The resulting model, which we refer to as mPLUG2+, consists of a CLIP-based video encoder and a Llama-based text decoder, totaling 1.4B parameters. We fine-tune the model on video captioning datasets to align the visual and text components; script generation requires no additional training. Compared to the original mPLUG2, this update improves captioning (by 2.8–3.7 CIDEr) and retrieval (by 3.8–4.9 Recall@1) performance, as shown in Section 5.2. To support reuse-centric execution, each module is serialized independently and kept persistently loaded during pipeline execution. This design enables both shared reuse and thread-safe parallelism across subtasks, enabling reliable execution on mobile devices with 6GB+ RAM.

**Adaptability to Other VLMs.** While our implementation uses mPLUG2+ as the base model, ATOM’s reuse-centric design is broadly compatible with many modern VLMs that follow a modular architecture, such as BLIP-2, Flamingo, and VideoCoCa. These models decouple video encoders and language decoders, making them suitable for persistent

reuse. Although earlier tightly coupled models with joint cross-modal attention layers may resist such decomposition, deployment on mobile devices generally necessitates modularization for latency and memory efficiency, an assumption increasingly reflected in newer model architectures.

**Quantization.** To support deployment on memory-constrained mobile hardware, we apply model quantization to reduce the memory footprint. We apply dynamic quantization using TorchAO to enable efficient deployment of our video-language models on mobile devices. Focusing on Linear and Embedding layers (responsible for over 91% of memory use), we achieve int8 compatibility and serialization for ARM CPUs while avoiding unreliable Conv3D quantization. Details of quantization, operator compatibility, serialization, and deployment constraints are included in Appendix C and D.

## 5 Results and Discussion

We evaluate ATOM on two representative video-language pipelines (video assembly and video retrieval) demonstrating the following key findings: (a) The modified mPLUG2+ architecture supports task reuse without performance degradation; and (b) ATOM’s reuse-centric design substantially reduces end-to-end latency by avoiding repeated weight loading and enabling parallelism.

We begin by detailing our experimental setup in Section 5.1, followed by results and analysis in Sections 5.2 and 5.3. Additional qualitative examples and results are provided in Appendix E and F.

### 5.1 Experimental Setup

**Tasks and Models.** We choose video retrieval and video assembly to represent two ends of the video-language task spectrum: retrieval-based reasoning and generative storytelling. Despite their differences, both benefit from caption generation as a shared intermediate step. This enables us to reuse the same language decoder across tasks, reducing latency and memory spent in the model loading phase. While server-side systems may afford task-specific models, our design favors reuse to meet mobile constraints. Appendix B discusses how this approach extends to other tasks like summarization.

Both pipelines rely on three core modules: a visual encoder for video encoding, a language decoder for caption generation (conditioned on video features), and a sentence transformer for matching user prompts to generated captions. The language decoder is also reused for script generation, enabling efficiency in ATOM’s reuse-centric design.

As described in Section 4, we use CLIP-ViT/L-14 (0.4B parameters) as the visual encoder and Llama 3.2 (1B parameters) as the language decoder. The model is fine-tuned for video captioning using four NVIDIA A100 GPUs and the datasets described below. For semantic matching, we use all-MiniLM-L6-v2 (Reimers and Gurevych 2019), a 22.7M parameter sentence transformer.

**Datasets.** We use three datasets to fine-tune and evaluate the modified mPLUG2+ for video captioning, video

retrieval, and qualitative video assembly (Appendix E): (a) MSR-VTT (Xu et al. 2016), (b) MSVD (Chen and Dolan 2011), and (c) DiDeMo (Hendricks et al. 2018). The model is trained on the combined training splits of all three datasets and evaluated on their respective test sets. The first two were also used in training the original mPLUG2.

MSR-VTT contains 10K YouTube videos with 200K captions, split into 6.5K training, 0.5K validation, and 3K test samples. MSVD has 1,970 YouTube clips with captions, divided into 1.2K/100/670 training/val/test samples. DiDeMo includes 10K Flickr videos, split into 8K/1K/1K, each paired with four text descriptions.

**Counterparts for Comparison.** Prior works on video assembly (Yang et al. 2023; Yin et al. 2024) rely on human-written scripts to retrieve relevant clips. In contrast, ATOM generates scripts from video clips based on user prompts. These prior systems are also closed-source, preventing reproducible comparisons. For video retrieval, existing methods focus on (a) architectural advances (Xu et al. 2023c,b) or (b) improving retrieval relevance (Tevissen, Guetari, and Petitpont 2024), but those designed for mobile settings (Zhang et al. 2021; Tahboub, Gadgil, and Delp 2015) do not leverage large language models for reasoning.

Due to these limitations, we evaluate ATOM using system-level baselines focused on performance and efficiency: (a) a 96-core x86\_64 CPU server, both with and without ATOM’s reuse-centric design; (b) the same server equipped with an NVIDIA A40 GPU, evaluated in both quantized and full-precision modes, again with and without reuse; and (c) ATOM on mobile devices without reuse, where separate models are loaded and unloaded for each subtask. The third baseline reflects typical multi-stage pipelines without coordination. Comparing against it isolates the benefits of ATOM’s modular reuse in latency and memory efficiency.

**Metrics.** For evaluating **video captioning subtask** performance, we employ four metrics: (a) BLEU@4, (b) ROUGE-L, (c) METEOR, and (d) CIDEr. BLEU@4 calculates the geometric mean of  $n$ -gram precision up to 4-grams between generated and reference captions, applying a brevity penalty. ROUGE-L assesses content overlap and word order by finding the longest common subsequence. METEOR computes a weighted harmonic mean of precision and recall, incorporating various linguistic features. CIDEr measures similarity using TF-IDF weighted cosine similarity of  $n$ -grams, emphasizing distinctive phrases. These metrics collectively provide a comprehensive assessment of caption quality, considering factors such as precision, recall, semantic similarity, and distinctiveness.

For evaluating **video retrieval task** performance, we use (a) Recall@1, (b) Recall@5, and (c) Recall@10. Recall@ $k$  measures the proportion of relevant videos successfully retrieved within the top  $k$  results of the video retrieval pipeline.

Meanwhile, the evaluation of **video assembly** has more human factors involved and there are no established metrics for the task. Hence we have performed qualitative analysis to measure efficacy of ATOM, as shown in Appendix E. For the task of **semantic matching** through sentence transformer, the metric of Pearson correlation measures the linear rela-

tionship between two sentence embeddings, quantifying semantic similarity based on how closely their values co-vary.

**Latency** is measured in seconds. We have measured the latency of loading model(s), running each component or a subtask (video encoding, caption generation) of a pipeline, as well as the latency of running the end-to-end pipeline. **Memory consumption** is measured in Gigabytes (GBs).

**Hardware.** We evaluated ATOM on 3 physical mobile devices with diverse computing capabilities: (a) Google Pixel 5a (6GB RAM), (b) Google Pixel 8a (8GB RAM), and (c) Samsung Galaxy S23 (8GB RAM). We have used Pytorch Mobile as the inference engine. Built for PyTorch Mobile, we also utilized TorchAO for optimized execution through operator fusion, quantization, and lightweight runtime adaptations. The experiments focused on executing the end-to-end task pipelines on mobile CPUs, given the limited compatibility of TorchAO (this limitation has been observed in other works as well (Xu et al. 2025, 2023a)) with alternative processing units such as GPUs and NPUs. However, ATOM remains adaptable to other processing units, making it orthogonal to the choice of hardware accelerators.

**Hyperparameters.** We follow the hyperparameters used for training mPLUG2 (Xu et al. 2023b). The training lasts for 10 epochs, with the learning rate of 2e-5 for the task of video description. The batch size is set to 128. The max caption generation length is set to 23 tokens, which is needed for fixing the decoding loop iterations of JIT tracing. Beam size of 4 is used for the caption generation. The videos are preprocessed to have sampling rate of 6 frames per second, and each frame’s resolution is decreased to 224×224. The hyperparameter selection is discussed in Appendix G.

## 5.2 Performance

In this section, we demonstrate the advantages of integrating a stronger language decoder in on-device video-language pipelines for retrieval and captioning tasks. Our enhanced mPLUG2+, powered by a LLaMa text decoder, delivers substantial gains in prediction performance compared to the original mPLUG2 with a BERT decoder, achieving 2.8–3.7 and 6.8–7.2 CIDEr point improvements without and with quantization, respectively. Moreover, quantization has a minimal impact on performance, causing only a 0.6–1.3 CIDEr reduction, while enabling efficient deployment on mobile and edge devices. These advancements allow us to build the first fully operable on-device video assembly pipeline, making real-time video understanding feasible.

We first discuss the performance of video captioning and video retrieval tasks, as detailed in Tables 1 and 2 respectively. Due to the lack of quantitative metrics for the video assembly task, we have conducted a qualitative analysis on the assembled videos with 10 human participants, those results are included in Appendix E.

Compared to the original mPLUG2, our modified mPLUG+ improves BLEU@4 by 1.9–5.5 points, indicating better alignment between generated captions and reference captions. It also achieves ROUGE-L gains of 2.3–2.8 points, reflecting improved phrase-matching accuracy, and METEOR gains of 2.1–2.6 points, which capture better

Model Variant	MSR-VTT				MSVD			
	B	R	M	C	B	R	M	C
Without Quantization (32-bit weights)								
mPLUG2	56.9	34.0	68.2	79.4	73.4	46.8	84.7	163.6
mPLUG2+	62.4	36.8	70.8	83.1	75.3	49.1	86.8	166.4
With Quantization (8-bit weights)								
mPLUG2	52.4	30.8	65.4	75.3	70.8	43.2	80.7	158.1
mPLUG2+	60.7	35.9	68.6	82.5	74.2	46.3	84.5	164.9

Table 1: **Performance** comparison of the original mPLUG2 (with BERT text decoder) and mPLUG2+ (with LLaMa text decoder) for both quantized and full-precision versions for the task of **video captioning**. All 4 metrics B (BLEU@4), R (ROUGE-L), M (METEOR), and C (CIDEr) are “higher the better”. mPLUG2+ of our method ATOM has a lower performance drop even after quantization, compared to the original mPLUG with a weaker text decoder.

word alignment. Furthermore, CIDEr, which measures caption informativeness, improves by 2.8–3.7 points. Even after quantization, mPLUG2+ consistently outperforms the original model by 6.8–7.2 CIDEr score. Due to quantization, we see a minor degradation of 0.6–1.5 CIDEr score compared to full-precision mPLUG+, while maintaining a negligible qualitative difference, as detailed in Appendix E.

Similarly, our retrieval results in Table 2 show consistent performance improvements across MSR-VTT, and MSVD datasets. Extended results on DiDeMo dataset are available in Appendix F.6. The full-precision mPLUG2+ model achieves Recall@1 gains of 3.8–4.9 points over mPLUG, demonstrating its stronger ability to retrieve the most relevant video. We observe similar trends for Recall@5 and Recall@10, reinforcing the robustness of our model across different ranking positions. Even with quantization, mPLUG2+ maintains a retrieval advantage over the original mPLUG2, with a Recall@1 drop of only 1.3–2.3 points, yet still outperforming the quantized mPLUG model by 4.7–7.1 points. Additionally, we show (in Appendix F.3) that the all-MiniLM-L6-v2 sentence transformer for caption-to-prompt matching in both retrieval and assembly pipelines has negligible impact on the end-to-end quality of our system, even after quantization. This ensures efficient and accurate matching in resource-constrained settings.

### 5.3 Latency

This section presents how the reuse-centric design for efficient pipeline execution of ATOM leads to latency reduction of 27–33% for video assembly and video retrieval tasks.

Table 3 shows that ATOM achieves substantial latency reductions across resource-constrained devices. On the Google Pixel 5a, our reuse-centric design lowers the end-to-end video retrieval latency by 33.06%, and video assembly latency by 30.78%. Similar trends are observed on the Google Pixel 8a and Samsung Galaxy S23, with latency reductions of approximately 30.43% and 29.14% for retrieval, and 27.69% and 27.54% for assembly, respectively. These

Model Variant	MSR-VTT			MSVD		
	R@1	R@5	R@10	R@1	R@5	R@10
Without Quantization (32-bit floating point weights)						
mPLUG2	52.6	75.8	83.1	65.3	82.0	90.6
mPLUG2+	57.2	80.7	85.1	69.1	84.5	93.8
With Quantization (8-bit integer weights)						
mPLUG2	48.7	72.6	80.5	62.1	77.3	87.9
mPLUG2+	55.8	78.4	82.9	66.8	82.7	90.3

Table 2: **Performance** comparison of the original mPLUG2 (with BERT text decoder) and our modified mPLUG2+ (with Llama text decoder) for both quantized and full-precision versions for the task of **video retrieval**. All 3 metrics R@1 (Recall@1), R@5 (Recall@5), and R@10 (Recall@10) are “higher the better”. mPLUG2+ of ATOM has a lower performance drop even after quantization, compared to the original mPLUG with a weaker text decoder.

reductions are driven by the parallel execution and amortized reuse of computational modules, significantly reducing redundant processing.

The key factor behind these improvements is ATOM’s ability to avoid repeated model loading and execution overhead. Traditional sequential, multi-model implementations reload models for different tasks, introducing substantial latency penalties, especially on mobile devices with constrained computational power. By reusing modules of a large video-language model, specifically our modified mPLUG2+, ATOM eliminates redundant computations and allows concurrent execution of different pipeline stages, leveraging hardware parallelism more effectively. This leads to noticeable latency reduction for video assembly and video retrieval, where sequential execution would otherwise introduce significant bottlenecks, as shown in “(w/o reuse)” counterparts of the table.

Another critical insight is the comparison between high-end server configurations and mobile hardware. While GPUs in high-end setups, such as the NVIDIA A40, greatly reduce latency through efficient vectorized computations, mobile devices lack such accelerations. In these environments, optimizing execution flow is even more crucial. The results confirm that ATOM’s reuse-focused approach is effective in bridging this performance gap, delivering end-to-end latency reductions exceeding 30% without requiring additional specialized hardware.

Furthermore, the impact of quantization on latency underscores the importance of ATOM’s design. While quantization generally reduces a model’s memory consumption, it introduces dynamic conversion overheads that can increase latency in implementations of video-based pipelines without reuse. However, ATOM mitigates this by parallelizing the execution on video encoder and language decoder, preventing performance degradation. The improvements are particularly evident in resource-constrained mobile device setups, where our approach prevents excessive delays caused by sequential processing of quantized operations.

	Platform Variant	Model Loading	Component-wise*				End-to-end	
			Video Encoding (CLIP-ViT)	Caption Generation (Llama)	Indexing (MiniLM)	Script Generation (ST + Decoder)	Video Retrieval	Video Assembly
Without Quantization								
	x86.64 CPU (w/o reuse)	6.19	1.68	1.15	10.35	11.09	36.05	40.67
	x86.64 CPU + GPU (w/o reuse)	8.66	0.15	0.08	6.48	6.84	12.12	14.95
	x86.64 CPU (ATOM)	3.44 (↓ 44.43%)	1.68	1.15	10.35	11.09	26.58 (↓ 26.27%)	30.28 (↓ 25.55%)
	x86.64 CPU + GPU (ATOM)	4.38 (↓ 49.42%)	0.15	0.08	6.48	6.84	8.65 (↓ 28.63%)	10.46 (↓ 30.03%)
With Quantization								
High-end Hardware	x86.64 CPU (w/o reuse)	7.32	2.95	2.14	13.66	15.40	44.84	47.59
	x86.64 CPU + GPU (w/o reuse)	8.89	0.46	0.32	10.78	13.02	19.20	22.18
	x86.64 CPU (ATOM)	3.64 (↓ 50.27%)	2.95	2.14	13.66	15.40	32.12 (↓ 28.37%)	34.69 (↓ 27.11%)
	x86.64 CPU + GPU (ATOM)	4.56 (↓ 48.71%)	0.46	0.32	10.78	13.02	14.02 (↓ 26.98%)	16.38 (↓ 26.15%)
Resource-constrained Hardware	Google Pixel 5a (w/o reuse)	32.94	8.68	5.57	24.39	26.61	162.33	167.52
	Google Pixel 8a (w/o reuse)	29.63	6.34	4.22	21.20	22.41	147.04	153.59
	Samsung Galaxy S23 (w/o reuse)	28.43	6.83	3.54	21.03	22.68	146.47	152.35
Hardware	Google Pixel 5a (ATOM)	17.23 (↓ 47.69%)	8.68	5.57	24.39	26.61	108.66 (↓ 33.06%)	115.95 (↓ 30.78%)
	Google Pixel 8a (ATOM)	15.87 (↓ 46.44%)	6.34	4.22	21.20	22.41	102.30 (↓ 30.43%)	111.06 (↓ 27.69%)
	Samsung Galaxy S23 (ATOM)	14.12 (↓ 50.33%)	6.83	3.54	21.03	22.68	103.78 (↓ 29.14%)	110.39 (↓ 27.54%)

Table 3: **Latency (in seconds, lower the better)** comparison of ATOM against a sequential (w/o reuse) implementation. The numbers in parentheses (↓) indicate the percentage savings of ATOM over the sequential baseline. The table reports both **component-wise latencies** of each subtask (video encoding, caption generation, indexing, and script generation) and **end-to-end latencies** for retrieval and video assembly tasks, on high-end servers and resource-constrained mobile devices. GPU: NVIDIA A40. \*Note: Component-wise latencies are measured independently per input. End-to-end latency, however, reflects execution over 5 inputs, showcasing the benefits of ATOM’s parallel execution and amortized model reuse. This design significantly reduces overall runtime by loading model modules only once and enabling concurrent processing across inputs, leading to end-to-end latencies lower than the naive sum of individual component times.

Overall, these findings validate the effectiveness of ATOM’s reuse-centric pipeline execution. By strategically leveraging modular reuse and concurrent execution, ATOM significantly accelerates video retrieval and assembly tasks, making real-time video processing feasible even on mobile hardware. The results highlight the importance of optimizing computational reuse to achieve low-latency, high-efficiency AI-driven applications.

#### 5.4 Additional Results

To further support the practical viability of ATOM, Appendix F provides results covering latency-performance trade-offs, storage feasibility, and memory efficiency.

(a) Ablation studies on a Google Pixel 5a in Appendix F.1 demonstrate the trade-offs between latency and performance under different execution configurations, including video resolution, caption length, frame rate, beam size, and batch size. These allow practitioners to adapt the system based on their specific deployment constraints.

(b) We also analyze model storage feasibility in Appendix F.2. The modularized video-language model, including the SentenceTransformer, occupies  $\sim 1.3$ GB in total; making it practical for deployment on typical smartphones with 6–8GB of RAM.

(c) Finally, Appendix F.4 and F.5 provides a detailed memory breakdown of ATOM compared to a non-reuse variant, and a discussion on latency-memory trade-off. Because ATOM holds the encoder and decoder in memory while they

execute in parallel, activation footprint rises by 182MB, but this is offset by the elimination of temporary buffers created during repeated model loading. The net effect is a negligible 0.76% ( $\approx 40$ MB) increase in peak RAM, leaving the complete pipeline well within the 6GB budget of commodity smartphones.

## 6 Conclusion

In this work, we present ATOM, an efficient on-device system that enables end-to-end video-language pipelines on commodity mobile devices. ATOM adopts a reuse-centric design that modularizes and repurposes components of a single VLM to serve all stages of the pipeline. This approach not only addresses critical challenges of model loading latency, but also ensures practical deployment on devices with as little as 6GB of RAM. Our evaluations across commercial smartphones demonstrate that – compared to de facto sequential, multi-model pipelines with no modularization or reuse – ATOM achieves stronger performance (up to 3.7 CIDEr score for assembly and 4.9 Recall@1 for retrieval) on downstream tasks with minimal degradation due to quantization, while significantly improving runtime efficiency (up to 33%). The qualitative evaluation echoes the quantitative gains of ATOM. By eliminating the need for external servers, ATOM enhances privacy, reduces infrastructure costs, and makes advanced video-language applications accessible even in bandwidth-constrained or offline environments.

## A Use Case: Video Assembly

We detail how ATOM executes the video assembly task entirely on-device, showcasing its modular and reuse-centric design. This example highlights the pipeline architecture and the interaction between the video encoder and language decoder modules.

### A.1 Pipeline Overview

Given a user prompt (e.g., “make a highlight reel”) and a set of user-provided videos, the pipeline proceeds as follows:

1. **Video segmentation.** Input videos are divided into overlapping clips of fixed duration ( $\ell = 10s$ ) with a stride of  $s = 5s$ , enabling finer temporal granularity and reducing memory load per inference call.
2. **Video captioning.** Each clip is passed through the VLM in a two-stage process:
  - The video encoder extracts high-dimensional visual embeddings.
  - The text decoder generates a concise natural language caption from the visual embedding.
3. **Embedding and ranking.** Captions and the user prompt are embedded using a Sentence Transformer. Clip relevance is computed via cosine similarity between caption and prompt embeddings.
4. **Script generation.** The top- $k$  relevant captions are composed into a coherent video script using the same VLM text decoder, now operating in text-only mode. This script determines the selected clip order and narration.
5. **Final assembly.** Selected clips are stitched together on-device into the final video output.

### A.2 Preprocessing for Mobile Constraints

To reduce inference latency and memory overhead, we preprocess video clips using the following strategies:

- **Resolution and frame rate reduction.** We downsample smartphone video input in both spatial and temporal dimensions.
- **Clip formatting.** Each video clip is reshaped to a tensor of size  $(1, 3, 6, 224, 224)$ , corresponding to batch size, channels, sampled frames, height, and width. This size achieves a good trade-off between accuracy and efficiency for scene-level understanding.

The entire pipeline, from segmentation to script generation, runs fully on-device, benefiting from persistent module reuse to avoid unnecessary reloading. Figure 1 in the main paper visualizes this process.

## B Broader Applicability to Video-Language Tasks

While video assembly is our primary case study, the reuse-centric architecture of ATOM generalizes naturally to a wide range of video-language tasks, including video retrieval, summarization, question answering, and more. These applications share a common multi-stage structure: they require video encoding followed by language-based reasoning

or matching, making them well-suited for ATOM’s modular, persistent, and parallel execution design.

In video retrieval, each clip is first processed by the visual encoder to produce embeddings. Instead of storing high-dimensional latent representations (e.g.,  $2048 \times 1024$ , which can occupy up to 8MB per clip), ATOM uses the language decoder to generate compact, semantically rich textual descriptions. This text-based representation reduces storage overhead to just a few hundred bytes per clip, and facilitates fast similarity-based matching using a lightweight sentence transformer model (e.g., all-MiniLM-L6-v2,  $\sim 90$ MB). The reuse-centric pipeline reuses both the visual encoder and the language decoder across all retrieval steps, eliminating redundant model loading and significantly reducing latency and memory usage. This makes accurate video retrieval feasible even on memory-constrained mobile devices.

In video summarization, the model first generates scene-level captions for short video segments using the encoder-decoder pair. These intermediate captions are then passed back into the same language decoder to generate higher-level summaries. Because the decoder remains loaded in memory from the initial captioning step, the summarization stage incurs no additional model load, leading to improved efficiency and consistent semantic representations across stages. This reuse not only reduces overhead but also supports coherent output quality through the use of a single, high-capacity decoder across all stages.

For video-based question answering (VideoQA), the video is again segmented and captioned using the visual encoder and decoder. Given a user question, the decoder then performs reasoning based on either the generated captions or raw visual embeddings to generate an answer. Since the decoder is already resident from earlier stages, it can be directly reused for reasoning without loading any QA-specific models, thereby lowering both latency and memory consumption.

Across all these applications, the key advantage of ATOM lies in its system-level reuse strategy. By maintaining loaded modules persistently in memory, ATOM avoids the need to load and unload models at each subtask boundary. This leads to consistent reductions in runtime and memory footprint while simplifying the software pipeline. Furthermore, by reusing the same language decoder across tasks; captioning, summarization, retrieval, and reasoning, ATOM ensures semantic consistency across outputs and avoids divergence that could arise from using separate specialized models.

The generality of this design supports a broader vision: modular and unified execution for a spectrum of video-language understanding tasks, optimized for on-device deployment. This makes ATOM not just a mobile-friendly architecture for video assembly, but a reusable backbone for future multimodal applications across edge devices.

## C Quantization

To enable deployment on commodity mobile hardware, we apply dynamic quantization to the video-language model components used in ATOM. Unlike previous work that focuses solely on shrinking model size for memory fit, our goal with quantization is to preserve runtime efficiency while

maintaining compatibility with mobile backends. This ensures that reused modules can remain persistently loaded and operate efficiently across tasks.

Quantizing video-language models presents several unique challenges. First, many popular quantization methods lack support for key operators used in video encoders, such as CONV3D. Additionally, some libraries fail to support int8 quantization or lack serialization capabilities necessary for ARM-based mobile deployment. Finally, quantization must be performed in a way that minimally impacts model accuracy.

To address these challenges, we adopt a dynamic quantization strategy using TORCHAO (torchao 2024). We target only the LINEAR and EMBEDDING layers, which together account for over 91% of model memory consumption. TORCHAO supports these operators and provides compatibility with ARM CPU execution through int8 datatypes. It also supports serialization, allowing us to package and deploy quantized models across a range of Android devices.

We deliberately exclude quantization of the CONV3D layers due to unreliable support across quantization libraries. Instead, we address the computational cost of video encoding through preprocessing, including frame rate and resolution downsampling prior to inference. This approach reduces runtime load without sacrificing too much fidelity in scene understanding.

In our evaluation, quantization introduces only a modest performance drop, approximately 1.5 CIDEr points on the captioning task and 2.3 Recall@1 on video retrieval, while enabling full pipeline deployment on devices with just 6GB of RAM. We also observe faster model load times and reduced peak memory usage, which further improve end-to-end latency.

It is worth emphasizing that quantization in ATOM complements our core design goal: reducing runtime overhead through architectural reuse. Our contribution is not in developing new quantization methods, but in ensuring that standard techniques like dynamic quantization can be integrated seamlessly into a reuse-centric execution model, enabling persistent in-memory operation of high-capacity modules under mobile constraints.

## D Serializing and Deploying the Quantized Model

On resource-constrained devices such as mobile phones, storing and deploying quantized models differs significantly from Python-based execution on high-end servers, where model weights are typically stored as a dictionary. For mobile deployment, the quantized model must be serialized by tracing its entire forward pass, including nested forward passes across multiple modules. This approach ensures compatibility with mobile execution environments and supports efficient inference on constrained hardware.

To enable saving and loading of quantized video-language models, we employed `torch.jit.trace`, which records the operations executed during a forward pass into a computational graph. However, several refactors were required to ensure compatibility:

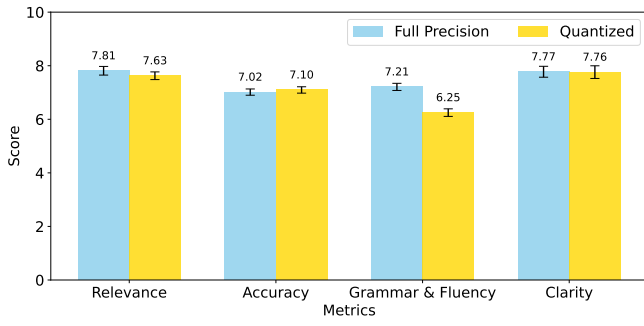
1. **Statically-typed Forward Passes:** The PyTorch JIT (just-in-time) compiler struggles with dynamic datatype inference during variable assignments and conditional operations. We refactored all forward passes in the sub-modules (visual encoder, and text decoder) to use static typing.
2. **Data-dependent Control Flows:** Tracing the text decoder proved challenging due to its inability to handle dynamic output lengths. As a workaround, we used sample inputs generating the maximum caption length and trimmed any excess tokens from the output.
3. **Substitute Torch Operations:** Certain matrix operations, such as `torch.rsub` and `torch.zeros`, are incompatible with JIT tracing. We replaced these with equivalent operations, such as combining `torch.mul` and `torch.sub`, or using `torch.zeros_like`.

Following the tracing of the forward pass, we applied additional optimizations tailored for mobile deployments. These include: (a) **Operator Fusion:** We merged the kernels of frequently paired operations, such as LINEAR and RELU, to reduce execution overhead and enhance runtime efficiency. (b) **Parameter Hoisting:** To minimize the storage of structural metadata, we restructured the model by hoisting all operators to the top level of the forward pass, streamlining execution and reducing the overall memory footprint. These optimizations further improve the efficiency and feasibility of deploying quantized video-language models on resource-constrained mobile devices.

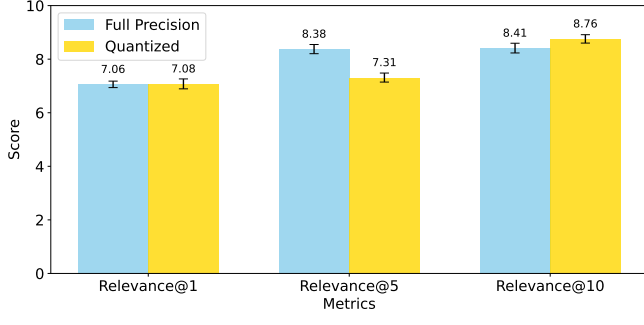
## E Qualitative Analysis

With 10 human participants, we have evaluated the performance of video captioning, video retrieval, and video assembly tasks on the full-precision and quantized versions of ATOM’s modified mPLUG2+. The results are shown in Figure 3. The qualitative metrics have scores from 0 (low score for the corresponding metric) to 10 (high score for the corresponding metric). The observed results related to the scores are discussed next.

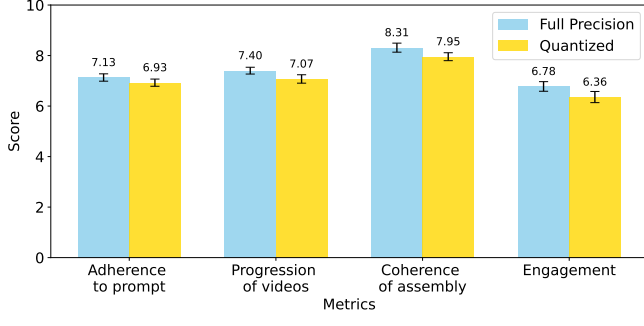
For the task of video captioning, we evaluated the generated captions on (a) Relevance: whether the caption is appropriate for the theme or essence of the video, (b) Accuracy: whether the caption has correct details about the objects present in the video, (c) Grammar and fluency: the linguistic correctness and naturalness of the caption, and (d) Clarity: whether the caption is unambiguous. Each participant was shown 10 videos with the captions generated from both the full-precision and quantized models. Figure 3a presents the mean scores for the evaluated metrics, with error bars indicating standard deviation. The mean participant-assigned scores for full-precision and quantized models differ by 0.1-1 across the four metrics. The standard deviation of these scores ranges from 0.7 to 1.2 for both models, suggesting that the observed mean differences are statistically insignificant. Consequently, the results indicate a negligible difference in caption quality between full-precision and quantized models; echoing the quantitative results shown in Table 1. Small samples of the generated captions are shown in Table 4, corroborating the negligible differences between



(a) Video captioning



(b) Video retrieval



(c) Video assembly

Figure 3: Qualitative analysis of the three tasks: (a) video captioning, (b) video retrieval, (c) video assembly. The results are based on 10 participants. The scale of different metric scores is [0, 10].

the generation capabilities of the full-precision and quantized models.

In context of the task of video retrieval, we evaluated the retrieved videos (given a prompt) on Relevance at top- $k$  (Relevance@ $k$ ) by showing them top- $k$  video(s) and asking how appropriate the video content is to the written prompt. Each participant was asked to write 10 prompts and evaluate the top-1, top-5, and top-10 relevance on the videos retrieved by both the full-precision and quantized models. Figure 3b shows the mean scores for the above metrics, with error bars showing standard deviation. The mean top- $k$  scores across all participants are in the range of 0.10-1.52 between full-precision and quantized models. The standard deviation is in the range of 0.75-1.02 for the full-precision model, and

in the range of 0.92-1.13 for the quantized model. The results indicate that the mean top- $k$  scores for full-precision and quantized models fall within a similar range, with overlapping standard deviations. This suggests that quantization has minimal impact on video retrieval performance, as both models exhibit comparable score distributions.

Lastly, for the task of video assembly, the qualitative evaluation is based on (a) Adherence to the prompt: Whether the content of the assembled video matched the given prompt, (b) Progression of videos: Whether the sequence of videos in the assembly seems to be in a natural order, (c) Coherence of the assembly: Whether the style and content of the assembled video clips make sense together, and (d) Engagement: How interesting or compelling the assembled video is. Each participant was asked to write 10 prompts and evaluate the above metrics on the videos assembled by both the full-precision and quantized models. Figure 3c shows the mean scores for the above metrics, with error bars showing standard deviation. The mean scores for the full-precision model range from 6.8 to 8.3, while the quantized model scores range from 6.3 to 7.9. The standard deviation is between 0.81-1.17 for the full-precision model and between 0.77-1.19 for the quantized model. The overlapping standard deviations suggest that quantization has a negligible impact on the task of video assembly too, as both models yield similar score distributions.

Therefore, across all three tasks – video captioning, video retrieval, and video assembly – the qualitative evaluation shows that quantization has minimal impact on performance, with mean scores and standard deviations exhibiting significant overlap between full-precision and quantized models.

## F Additional Results

In this section, we present additional results that provide deeper insight into our system’s efficiency and design choices, including ablation studies, storage requirements, quantization effects, and memory footprint analysis.

### F.1 Ablation Studies

Table 5 demonstrates the impact of varying input configurations and hyperparameters on the latency and performance of ATOM’s modified mPLUG2+ on a Google Pixel 5a. The default configuration (1, 3, 6, 224, 224) achieves a latency of 5.75s and a CIDEr score of 82.5, providing a baseline for comparison.

(i) **Adjusting the traced output length** to 12 reduces latency to 4.55s, but lowers the CIDEr score to 74.19, as shorter outputs often fail to capture the full detail of ground truth captions. (ii) **Lowering the input frame rate (FPS)** from 6 to 2 reduces latency to 4.78s, but leads to a significant drop in performance (CIDEr: 50.89) due to insufficient temporal coverage. (iii) **Reducing the frame resolution** to (112, 112) lowers latency to 3.29s, with only a mild performance loss (CIDEr: 75.64), highlighting an effective trade-off. (iv) **Reducing the beam size** to 1 yields a latency of 3.07s, but severely degrades performance (CIDEr: 40.98) due to limited search diversity during generation. (v) **Increasing the batch size** to 4 increases latency to 22.35s,

#	Caption generated by the original full-precision (float32) model	Caption generated by the quantized quantized (int8) model
1	a person is wrapping gifts	a person is wrapping gifts
2	showing a cityscape to the camera	a city is being shown
3	a person is making a tortilla	a person is making a tortilla
4	a woman unpacks a box	a woman opens a box
5	a woman is opening a box	a person is opening a box
6	a woman is praying	a woman is putting candles on a statue
7	a girl is reading a book	a girl is reading a book
8	a woman is reading a book	a woman is reading
9	showing a photo of street fair to the camera	footage of a carnival
10	turning the camera upwards while filming a city	turning the camera upwards while filming a city
11	a group of people are playing instruments outside	a group of people are singing and playing instruments
12	a person is cooking	a person is cooking

Table 4: Comparison of the captions (text descriptions of the videos) generated by the original full-precision float32 mPLUG model and the quantized int8 video-language model (modified mPLUG2+). We see minute but synonymous differences, indicating that the quality of the captions are preserved after quantization.

Input Shape (Batch size, Channels, FPS, Width, Height)	Latency	CIDEr Score
(1, 3, 6, 224, 224): default case	5.57	82.5
(1, 3, 2, 224, 224)	4.78	50.89
(1, 3, 6, 112, 112)	3.29	75.64
(4, 3, 6, 224, 224)	22.35	82.5
(1, 3, 6, 224, 224): generator beam size = 1	3.07	40.98
(1, 3, 6, 224, 224): traced output length = 12	4.55	74.19

Table 5: Changing input sizes and hyperparameters to measure their impact on latency and performance. All experiments are measured on Google Pixel 5a for the task of video assembly with the test dataset of MSR-VTT. The default input shape is (1, 3, 6, 224, 224), with traced output length of 23 and generated beam size of 4.

while maintaining the same CIDEr score (82.5) as the default, illustrating that batching offers no speed advantage on constrained hardware. These results emphasize the importance of tuning both inputs and decoding settings to balance latency and quality, particularly in mobile deployment scenarios.

## F.2 Storage Size

Table 6 shows that the combined storage size of the video-language model mPLUG+ and sentence transformer all-MiniLM-L6-v2 is 1.28GB, with the video-language model accounting for 1.23GB and the sentence transformer for 53MB. This compact size ensures that the models are feasible to store on most commodity smartphones, enabling on-device deployment of end-to-end pipelines for video captioning and retrieval.

	Storage Size (in MBs)
Video-Language Model (mPLUG+)	1230
Sentence Transformer (all-MiniLM-L6-v2)	53
Total	1283

Table 6: **Storage size (in MBs)** of the video-language model and sentence transformer used for end-to-end task pipelines of **video assembly**, **video captioning** and **video retrieval**. The total storage size required for the pipelines is 1.28GB, which is feasible for the most commodity smartphones.

## F.3 Quantizing the Sentence Transformer

Table 7 shows that the full-precision version of all-MiniLM-L6-v2 SentenceTransformer has a Pearson Correlation of 0.83 on the test partition of Semantic Textual Similarity Benchmark (STS-B) dataset. The quantized version minutely underperforms with the Pearson Correlation of 0.81, however the qualitative analysis (in Appendix E) shows that the impact of such performance drops due to quantization is negligible on the end-to-end performance.

## F.4 Memory Footprint

The goal of this section is to quantify the memory footprint of ATOM and show that its reuse-centric design does not exceed the tight RAM budgets of mobile devices. Table 8 reports the peak memory usage of the video-language pipeline with and without modular reuse. The two configurations differ by only 40MB: 5.28GB for the baseline versus 5.32GB for ATOM, a negligible 0.76% increase that still fits comfortably within the 6 GB RAM of mainstream smartphones. The extra 40MB are due to the activations being slightly higher under ATOM (0.479GB vs. the sequential baseline’s 0.297GB) because the encoder and decoder can be active at the same time. This is offset by a sharp drop in the miscellaneous allocations, which are the temporary buffers created during model loading. The max memory consump-

SentenceTransformer Variant	Pearson Correlation ( $\uparrow$ )
Full-precision	0.8287
Quantized	0.8156

Table 7: Performance comparison of the full-precision and quantized versions of the sentence transformer `all-MiniLM-L6-v2` on Semantic Textual Similarity Benchmark (STS-B) dataset. The sentence transformer is used in our mobile pipelines to find text representation of the most relevant videos to a user query. We see a minor performance drop with the quantized version. While ATOM can accommodate the full-precision model in a mobile pipeline, we observe no end-to-end performance drop with the quantized sentence transformer.

	Max Memory Consumption (in GBs)	
	ATOM without modularization	ATOM and reuse
Model Weights	4.623	4.623
Inputs	0.005	0.005
Activations (highest across all the models or modules)	0.297	0.479
Miscellaneous (temporary variables in model loads)	0.352	0.210
Peak Memory Consumption for One Run of the Pipeline	5.277	5.317

Table 8: **Memory Consumption (in GBs, lower the better)** of the video-language model used for the task pipeline of **video assembly**. The pipeline with ATOM consumes 5.3GBs of RAM for ATOM, which is feasible to run for recent commodity smartphones having 6GB of RAM. ATOM only incurs 0.76% more memory usage compared to the implementation without modularization and reuse, due to the elimination of 40.34% of the temporary allocations created during model loading.

Module Name	Parameter Count	Parameter Size (in MBs)	% of Total Size
LINEAR	1236M	3689	80.82%
EMBEDDING	161M	487	10.67%
CONV3D	51M	194	4.25%
NONDYNAMICALLY QUANTIZABLE LINEAR	49M	193	4.22%
LAYERNORM	0.4M	2	0.04%

Table 9: Layer-wise breakdown of peak memory consumption for mPLUG2+.

tion related to the temporary allocations shrink by 40.34% (ATOM’s 0.210GB vs. the sequential baseline’s 0.352GB), due to keeping the heavy modules permanently resident. Model weights and input memory remain identical across the two variants.

**Latency–memory trade-off.** Although ATOM sacrifices a 40MB extra RAM to enable parallelism, it delivers 27–33% end-to-end latency reductions (see Section 5.3), making the trade-off highly favorable. Tighter memory savings would require pushing quantization beyond 8-bit, which we found degrades accuracy unacceptably. Instead, ATOM prioritizes reuse to maximize speed while remaining within the practical 6GB envelope of commodity phones.

## F.5 Layerwise Memory Breakdown

This section provides a finer-grained analysis of memory consumption across different layers of the video-language model mPLUG2+ used in ATOM. This breakdown enabled the identification of the dominant contributors to the total memory footprint. Understanding this breakdown is essential for targeting further optimizations.

Table 9 shows that the LINEAR and EMBEDDING layers dominate memory usage, consuming 80.82% (3,689MB) and 10.67% (487MB) of the total size, respectively. These layers, which are extensively used in the text decoder, present significant optimization opportunities.

By reusing the text decoder, ATOM effectively reduces both memory consumption and execution latency, demonstrating the efficiency of this architectural choice. This insight reinforces the importance of targeted optimizations in deep learning pipelines for resource-constrained environments.

## F.6 Extended Results: Video Retrieval on DiDeMo dataset.

To complement the main table on the video retrieval performance (Table 2) in Section 5.2, Table 10 presents the full DiDeMo retrieval results, highlighting how mPLUG2+ maintains strong performance even under quantization.

## F.7 Estimated Energy Consumption on Pixel 5a

To quantify the energy efficiency benefits of ATOM on a commodity mobile device, here we compute the reduction in energy consumption during video-language processing on the Google Pixel 5a.

Model Variant	DiDeMo		
	R@1	R@5	R@10
Without Quantization (32-bit floating point weights)			
mPLUG2	55.1	78.3	84.6
mPLUG2+	60.0	86.2	90.1
With Quantization (8-bit integer weights)			
mPLUG2	53.7	75.1	80.8
mPLUG2+	58.7	83.1	88.4

Table 10: **Performance** comparison of the original mPLUG2 (with BERT text decoder) and our modified mPLUG2+ (with Llama text decoder) for both quantized and full-precision versions for the task of **video retrieval** on DiDeMo dataset. All 3 metrics R@1 (Recall@1), R@5 (Recall@5), and R@10 (Recall@10) are “higher the better”. mPLUG2+ of ATOM has a lower performance drop even after quantization, compared to the original mPLUG with a weaker text decoder.

- **CPU Power:** The Pixel 5a’s Snapdragon 765G CPU draws approximately 2 Watts under moderate computational load typical of video-language model inference.
- **DRAM Power:** Active memory power consumption for LPDDR4X RAM is roughly 0.2 Watts at 6GB utilization during active workloads.
- **Latency:** The original pipeline execution latency is  $T_{\text{orig}} = 10$  seconds (example value). ATOM reduces latency by 27–33%, yielding a new latency  $T_{\text{new}} \approx 6.7\text{--}7.3$  seconds.
- **Memory Footprint:** ATOM’s peak RAM usage is essentially unchanged: 5.277GB (baseline) versus 5.317GB (+0.76%). The 0.76% increase is small enough that we assume DRAM power remains at 0.2W.

#### Calculation:

$$\begin{aligned} \text{Original Energy} &= (P_{\text{CPU}} + P_{\text{DRAM}}) \times T_{\text{orig}} \\ &= (2.0 \text{ W} + 0.2 \text{ W}) \times 10 \text{ s} = 22 \text{ J} \end{aligned}$$

$$\begin{aligned} \text{Adjusted CPU Power} &= 2.0 \text{ W} \times (1 - 0.27) \approx 1.46 \text{ W} \\ &\quad (\text{assuming CPU power scales with latency}) \end{aligned}$$

$$\text{Adjusted DRAM Power} = 0.2 \text{ W} \times (1 - 0.057) \approx 0.19 \text{ W}$$

$$\begin{aligned} \text{New Energy} &= (1.46 \text{ W} + 0.19 \text{ W}) \times 7.0 \text{ s} \\ &= 11.9 \text{ J} \end{aligned}$$

$$\therefore \text{Energy Savings} = \frac{22 - 11.9}{22} \times 100\% \approx 46\%$$

This estimate assumes linear scaling of CPU power with latency reduction and memory power with memory footprint reduction, which is reasonable for short, compute-bound workloads.

**Implications:** Reducing energy consumption by nearly half per pipeline execution can significantly extend battery

life during repeated video-language tasks. Most of the savings stem from ATOM’s reuse-centric design that trims CPU active time; memory power remains virtually unchanged because the peak footprint grows by only 0.76%.

#### G Hyperparameter Selection.

In order to train mPLUG2+ model on caption generation task, we had conducted a grid search over learning rates  $\{1e-3, 1e-4, 1e-5, 2e-5, 5e-5, 1e-6\}$  and found  $2e-5$  to yield the best tradeoff between stability and performance. Training beyond 10 epochs led to overfitting, so we used the checkpoint at epoch **10**. Batch sizes of  $\{32, 64, 128, 256\}$  were also evaluated; the batch size of 128 provided the best balance between training time and CIDEr score. The impact of other video-related hyperparameters is analyzed in the ablation study (Appendix F.1).

## References

Bain, M.; Nagrani, A.; Varol, G.; and Zisserman, A. 2021. Frozen in Time: A Joint Video and Image Encoder for End-to-End Retrieval. In *IEEE International Conference on Computer Vision*.

Chen, D. L.; and Dolan, W. B. 2011. Collecting Highly Parallel Data for Paraphrase Evaluation. In *Proceedings of the 49th Annual Meeting of the Association for Computational Linguistics (ACL-2011)*.

Chen, T.-S.; Siarohin, A.; Menapace, W.; Deyneka, E.; Chao, H.-w.; Jeon, B. E.; Fang, Y.; Lee, H.-Y.; Ren, J.; Yang, M.-H.; et al. 2024. Panda-70m: Captioning 70m videos with multiple cross-modality teachers. In *Proceedings of the IEEE/CVF Conference on Computer Vision and Pattern Recognition*.

Chu, X.; Qiao, L.; Lin, X.; Xu, S.; Yang, Y.; Hu, Y.; Wei, F.; Zhang, X.; Zhang, B.; Wei, X.; et al. 2023. Mobilevlm: A fast, reproducible and strong vision language assistant for mobile devices. *arXiv preprint arXiv:2312.16886*.

Grattafiori, A.; Dubey, A.; Jauhri, A.; Pandey, A.; Kadian, A.; Al-Dahle, A.; Letman, A.; Mathur, A.; Schelten, A.; Vaughan, A.; Yang, A.; Fan, A.; Goyal, A.; Hartshorn, A.; Yang, A.; Mitra, A.; Srivankumar, A.; Korenev, A.; Hinsvark, A.; Rao, A.; Zhang, A.; Rodriguez, A.; Gregerson, A.; Spataru, A.; Roziere, B.; Biron, B.; Tang, B.; Chern, B.; Caucheteux, C.; Nayak, C.; Bi, C.; Marra, C.; McConnell, C.; Keller, C.; Touret, C.; Wu, C.; Wong, C.; Ferrer, C. C.; Nikolaidis, C.; Allonsius, D.; Song, D.; Pintz, D.; Livshits, D.; Wyatt, D.; Esiobu, D.; Choudhary, D.; Mahajan, D.; Garcia-Olano, D.; Perino, D.; Hupkes, D.; Lakomkin, E.; AlBadawy, E.; Lobanova, E.; Dinan, E.; Smith, E. M.; Radenovic, F.; Guzmán, F.; Zhang, F.; Synnaeve, G.; Lee, G.; Anderson, G. L.; Thattai, G.; Nail, G.; Mialon, G.; Pang, G.; Cucurell, G.; Nguyen, H.; Korevaar, H.; Xu, H.; Touvron, H.; Zarov, I.; Ibarra, I. A.; Kloumann, I.; Misra, I.; Evtimov, I.; Zhang, J.; Copet, J.; Lee, J.; Geffert, J.; Vranes, J.; Park, J.; Mahadeokar, J.; Shah, J.; van der Linde, J.; Billock, J.; Hong, J.; Lee, J.; Fu, J.; Chi, J.; Huang, J.; Liu, J.; Wang, J.; Yu, J.; Bitton, J.; Spisak, J.; Park, J.; Rocca, J.; Johnstun, J.; Saxe, J.; Jia, J.; Alwala, K. V.; Prasad, K.; Upasani, K.; Plawiak, K.; Li, K.; Heafield, K.; Stone, K.; El-Arini, K.; Iyer, K.; Malik, K.; Chiu, K.; Bhalla, K.; Lakhotia, K.; Rantala-Yeary, L.; van der Maaten, L.; Chen, L.; Tan, L.; Jenkins, L.; Martin, L.; Madaan, L.; Malo, L.; Blecher, L.; Landzaat, L.; de Oliveira, L.; Muzzi, M.; Pasupuleti, M.; Singh, M.; Paluri, M.; Kardas, M.; Tsimpoukelli, M.; Oldham, M.; Rita, M.; Pavlova, M.; Kambadur, M.; Lewis, M.; Si, M.; Singh, M. K.; Hassan, M.; Goyal, N.; Torabi, N.; Bashlykov, N.; Bogoychev, N.; Chatterji, N.; Zhang, N.; Duchenne, O.; Çelebi, O.; Alrassy, P.; Zhang, P.; Li, P.; Vasic, P.; Weng, P.; Bhargava, P.; Dubal, P.; Krishnan, P.; Koura, P. S.; Xu, P.; He, Q.; Dong, Q.; Srinivasan, R.; Ganapathy, R.; Calderer, R.; Cabral, R. S.; Stojnic, R.; Raileanu, R.; Maheswari, R.; Girdhar, R.; Patel, R.; Sauvestre, R.; Polidoro, R.; Sumbaly, R.; Taylor, R.; Silva, R.; Hou, R.; Wang, R.; Hosseini, S.; Chennabasappa, S.; Singh, S.; Bell, S.; Kim, S. S.; Edunov, S.; Nie, S.; Narang, S.; Raparthy, S.; Shen, S.; Wan, S.; Bhosale, S.; Zhang, S.; Vandenhende, S.; Batra, S.; Whitman, S.; Sootla, S.; Collot, S.; Gururangan, S.; Borodinsky, S.; Herman, T.; Fowler, T.; Sheasha, T.; Georgiou, T.; Scialom, T.; Speckbacher, T.; Mihaylov, T.; Xiao, T.; Karn, U.; Goswami, V.; Gupta, V.; Ramanathan, V.; Kerkez, V.; Gonguet, V.; Do, V.; Vogeti, V.; Albiero, V.; Petrovic, V.; Chu, W.; Xiong, W.; Fu, W.; Meers, W.; Martinet, X.; Wang, X.; Wang, X.; Tan, X. E.; Xia, X.; Xie, X.; Jia, X.; Wang, X.; Goldschlag, Y.; Gaur, Y.; Babaei, Y.; Wen, Y.; Song, Y.; Zhang, Y.; Li, Y.; Mao, Y.; Coudert, Z. D.; Yan, Z.; Chen, Z.; Papakipos, Z.; Singh, A.; Srivastava, A.; Jain, A.; Kelsey, A.; Shajnfeld, A.; Gangidi, A.; Victoria, A.; Goldstand, A.; Menon, A.; Sharma, A.; Boessenberg, A.; Baevski, A.; Feinstein, A.; Kallet, A.; Sangani, A.; Teo, A.; Yunus, A.; Lupu, A.; Alvarado, A.; Caples, A.; Gu, A.; Ho, A.; Poulton, A.; Ryan, A.; Ramchandani, A.; Dong, A.; Franco, A.; Goyal, A.; Saraf, A.; Chowdhury, A.; Gabriel, A.; Bharambe, A.; Eisenman, A.; Yazdan, A.; James, B.; Maurer, B.; Leonhardi, B.; Huang, B.; Loyd, B.; Paola, B. D.; Paranjape, B.; Liu, B.; Wu, B.; Ni, B.; Hancock, B.; Wasti, B.; Spence, B.; Stojkovic, B.; Gamido, B.; Montalvo, B.; Parker, C.; Burton, C.; Mejia, C.; Liu, C.; Wang, C.; Kim, C.; Zhou, C.; Hu, C.; Chu, C.-H.; Cai, C.; Tindal, C.; Feichtenhofer, C.; Gao, C.; Civin, D.; Beaty, D.; Kreymer, D.; Li, D.; Adkins, D.; Xu, D.; Testuggine, D.; David, D.; Parikh, D.; Liskovich, D.; Foss, D.; Wang, D.; Le, D.; Holland, D.; Dowling, E.; Jamil, E.; Montgomery, E.; Presani, E.; Hahn, E.; Wood, E.; Le, E.-T.; Brinkman, E.; Arcaute, E.; Dunbar, E.; Smothers, E.; Sun, F.; Kreuk, F.; Tian, F.; Kokkinos, F.; Ozgenel, F.; Caggioni, F.; Kanayet, F.; Seide, F.; Florez, G. M.; Schwarz, G.; Badeer, G.; Sweene, G.; Halpern, G.; Herman, G.; Sizov, G.; Guangyi; Zhang; Lakshminarayanan, G.; Inan, H.; Shojanazeri, H.; Zou, H.; Wang, H.; Zha, H.; Habeeb, H.; Rudolph, H.; Suk, H.; Aspegren, H.; Goldman, H.; Zhan, H.; Damlaj, I.; Molybog, I.; Tufanov, I.; Leontiadis, I.; Veliche, I.-E.; Gat, I.; Weissman, J.; Geboski, J.; Kohli, J.; Lam, J.; Asher, J.; Gaya, J.-B.; Marcus, J.; Tang, J.; Chan, J.; Zhen, J.; Reizenstein, J.; Teboul, J.; Zhong, J.; Jin, J.; Yang, J.; Cummings, J.; Carvill, J.; Shepard, J.; McPhie, J.; Torres, J.; Ginsburg, J.; Wang, J.; Wu, K.; U, K. H.; Saxena, K.; Khandelwal, K.; Zand, K.; Matosich, K.; Veeraraghavan, K.; Michelena, K.; Li, K.; Jagadeesh, K.; Huang, K.; Chawla, K.; Huang, K.; Chen, L.; Garg, L.; A, L.; Silva, L.; Bell, L.; Zhang, L.; Guo, L.; Yu, L.; Moshkovich, L.; Wehrstedt, L.; Khabsa, M.; Avalani, M.; Bhatt, M.; Mankus, M.; Hasson, M.; Lennie, M.; Reso, M.; Groshev, M.; Naumov, M.; Lathi, M.; Keneally, M.; Liu, M.; Seltzer, M. L.; Valko, M.; Restrepo, M.; Patel, M.; Vyatskov, M.; Samvelyan, M.; Clark, M.; Macey, M.; Wang, M.; Hermoso, M. J.; Metanat, M.; Rastegari, M.; Bansal, M.; Santhanam, N.; Parks, N.; White, N.; Bawa, N.; Singhal, N.; Egebo, N.; Usunier, N.; Mehta, N.; Laptev, N. P.; Dong, N.; Cheng, N.; Chernoguz, O.; Hart, O.; Salpekar, O.; Kalinli, O.; Kent, P.; Parekh, P.; Saab, P.; Balaji, P.; Rittner, P.; Bontrager, P.; Roux, P.; Dollar, P.; Zvyagina, P.; Ratanchandani, P.; Yuvraj, P.; Liang, Q.; Alao, R.; Rodriguez, R.; Ayub, R.; Murthy, R.; Nayani, R.; Mitra, R.; Parthasarathy, R.; Li, R.; Hogan, R.; Battey, R.; Wang, R.; Howes, R.; Rinott, R.; Mehta, S.; Siby, S.; Bondu, S. J.; Datta, S.; Chugh, S.; Hunt, S.; Dhillon, S.; Sidorov, S.; Pan, S.; Mahajan, S.; Verma,

S.; Yamamoto, S.; Ramaswamy, S.; Lindsay, S.; Lindsay, S.; Feng, S.; Lin, S.; Zha, S. C.; Patil, S.; Shankar, S.; Zhang, S.; Zhang, S.; Wang, S.; Agarwal, S.; Sajuyigbe, S.; Chintala, S.; Max, S.; Chen, S.; Kehoe, S.; Satterfield, S.; Govindaprasad, S.; Gupta, S.; Deng, S.; Cho, S.; Virk, S.; Subramanian, S.; Choudhury, S.; Goldman, S.; Remez, T.; Glaser, T.; Best, T.; Koehler, T.; Robinson, T.; Li, T.; Zhang, T.; Matthews, T.; Chou, T.; Shaked, T.; Vontimitta, V.; Ajayi, V.; Montanez, V.; Mohan, V.; Kumar, V. S.; Mangla, V.; Ionescu, V.; Poenaru, V.; Mihailescu, V. T.; Ivanov, V.; Li, W.; Wang, W.; Jiang, W.; Bouaziz, W.; Constable, W.; Tang, X.; Wu, X.; Wang, X.; Wu, X.; Gao, X.; Kleinman, Y.; Chen, Y.; Hu, Y.; Jia, Y.; Qi, Y.; Li, Y.; Zhang, Y.; Zhang, Y.; Adi, Y.; Nam, Y.; Yu; Wang; Zhao, Y.; Hao, Y.; Qian, Y.; Li, Y.; He, Y.; Rait, Z.; DeVito, Z.; Rosnbrick, Z.; Wen, Z.; Yang, Z.; Zhao, Z.; and Ma, Z. 2024. The Llama 3 Herd of Models. *arXiv:2407.21783*.

Hendricks, L. A.; Wang, O.; Shechtman, E.; Sivic, J.; Darrell, T.; and Russell, B. 2018. Localizing Moments in Video with Temporal Language. In *Empirical Methods in Natural Language Processing (EMNLP)*.

Jeong, S.; Kim, K.; Baek, J.; and Hwang, S. J. 2025. Video-RAG: Retrieval-Augmented Generation over Video Corpus. *arXiv:2501.05874*.

Jo, W.; Lim, G.; Lee, G.; Kim, H.; Ko, B.; and Choi, Y. 2024. VVS: Video-to-Video Retrieval with Irrelevant Frame Suppression. *Proceedings of the AAAI Conference on Artificial Intelligence*, 38(3).

Li, G.; and Li, Y. 2023. Spotlight: Mobile UI Understanding using Vision-Language Models with a Focus. In *The Eleventh International Conference on Learning Representations*.

Long, X.; Ma, Z.; Hua, E.; Zhang, K.; Qi, B.; and Zhou, B. 2025. Retrieval-Augmented Visual Question Answering via Built-in Autoregressive Search Engines. In *Proceedings of the AAAI Conference on Artificial Intelligence*, volume 39.

Luo, H.; Ji, L.; Zhong, M.; Chen, Y.; Lei, W.; Duan, N.; and Li, T. 2021. Clip4clip: An empirical study of clip for end to end video clip retrieval. *arXiv preprint arXiv:2104.08860*.

Reimers, N.; and Gurevych, I. 2019. Sentence-BERT: Sentence Embeddings using Siamese BERT-Networks. In *Proceedings of the 2019 Conference on Empirical Methods in Natural Language Processing*. Association for Computational Linguistics.

Tahboub, K.; Gadgil, N. J.; and Delp, E. J. 2015. Content based video retrieval on mobile devices: How much content is enough? In *2015 IEEE International Conference on Image Processing (ICIP)*.

Tevissen, Y.; Guetari, K.; and Petitpont, F. 2024. Towards Retrieval Augmented Generation over Large Video Libraries. In *2024 16th International Conference on Human System Interaction (HSI)*.

torchao. 2024. TorchAO: PyTorch-Native Training-to-Serving Model Optimization.

Wang, Y.; Li, K.; Li, X.; Yu, J.; He, Y.; Chen, G.; Pei, B.; Zheng, R.; Wang, Z.; Shi, Y.; et al. 2024. Internvideo2: Scal-  
ing foundation models for multimodal video understanding. In *European Conference on Computer Vision*. Springer.

Wu, S.; Fei, H.; Qu, L.; Ji, W.; and Chua, T.-S. 2024. Nextgpt: Any-to-any multimodal Ilm. In *Forty-first International Conference on Machine Learning*.

Xu, D.; Yin, W.; Jin, X.; Zhang, Y.; Wei, S.; Xu, M.; and Liu, X. 2023a. LLMcad: Fast and Scalable On-device Large Language Model Inference.

Xu, D.; Zhang, H.; Yang, L.; Liu, R.; Huang, G.; Xu, M.; and Liu, X. 2025. Fast On-device LLM Inference with NPUs. *Proceedings of the 28th Annual International Conference on Mobile Computing And Networking*.

Xu, H.; Ye, Q.; Yan, M.; Shi, Y.; Ye, J.; Xu, Y.; Li, C.; Bi, B.; Qian, Q.; Wang, W.; Xu, G.; Zhang, J.; Huang, S.; Huang, F.; and Zhou, J. 2023b. mPLUG-2: a modularized multi-modal foundation model across text, image and video. In *Proceedings of the 40th International Conference on Machine Learning*.

Xu, J.; Lan, C.; Xie, W.; Chen, X.; and Lu, Y. 2023c. Retrieval-based Video Language Model for Efficient Long Video Question Answering. *arXiv:2312.04931*.

Xu, J.; Mei, T.; Yao, T.; and Rui, Y. 2016. MSR-VTT: A Large Video Description Dataset for Bridging Video and Language. *IEEE International Conference on Computer Vision and Pattern Recognition (CVPR)*.

Yan, D.; Li, P.; Li, Y.; Chen, H.; Chen, Q.; Luo, W.; Dong, W.; Yan, Q.; Zhang, H.; and Shen, C. 2025. TG-LLaVA: Text Guided LLaVA via Learnable Latent Embeddings. *Proceedings of the AAAI Conference on Artificial Intelligence*, 39.

Yang, G.; Lu, H.; Sun, Z.; and Lu, Z. 2023. Shot Retrieval and Assembly with Text Script for Video Montage Generation. In *Proceedings of the 2023 ACM International Conference on Multimedia Retrieval, ICMR '23*. Association for Computing Machinery.

Yin, Z.; Ma, Y.; Cao, X.; Wang, B.; Chen, Q.; and Jiang, P. 2024. Text-Video Multi-Grained Integration for Video Moment Montage. *arXiv:2412.09276*.

Zhang, H.; Jepson, A. D.; Mohomed, I.; Derpanis, K. G.; Zhang, R.; and Fazly, A. 2021. Personalized Multi-modal Video Retrieval on Mobile Devices. In *Proceedings of the 29th ACM International Conference on Multimedia, MM '21*. Association for Computing Machinery.